

1 **Air Quality and Climate Change, Topic 3 of the Model Inter-Comparison**
2 **Study for Asia Phase III (MICS-Asia III), Part II: aerosol radiative effects**
3 **and aerosol feedbacks**

4 Meng Gao¹, Zhiwei Han^{2,3}, Zhining Tao^{4,5}, Jiawei Li^{2,3}, Jeong-Eon Kang⁶, Kan Huang⁷, Xinyi
5 Dong⁸, Bingliang Zhuang⁹, Shu Li⁹, Baozhu Ge¹⁰, Qizhong Wu¹¹, Hyo-Jung Lee⁶, Cheol-Hee
6 Kim⁶, Joshua S. Fu⁸, Tijian Wang⁹, Mian Chin⁵, Meng Li¹², Jung-Hun Woo¹³, Qiang Zhang¹⁴,
7 Yafang Cheng¹², Zifa Wang^{3,10}, Gregory R. Carmichael¹⁵

8
9 1 Department of Geography, Hong Kong Baptist University, Hong Kong SAR, China
10 2 Key Laboratory of Regional Climate-Environment for Temperate East Asia, Institute of
11 Atmospheric Physics, Chinese Academy of Sciences, Beijing, China
12 3 University of Chinese Academy of Sciences, Beijing 100049, China
13 4 Universities Space Research Association, Columbia, MD, USA
14 5 NASA Goddard Space Flight Center, Greenbelt, MD, USA
15 6 Department of Atmospheric Sciences, Pusan National University, Busan, South Korea
16 7 Department of Environmental Science and Engineering, Fudan University, Shanghai, China
17 8 Department of Civil and Environmental Engineering, University of Tennessee, Knoxville,
18 TN, USA
19 9 School of Atmospheric Sciences, Nanjing University, Nanjing, China
20 10 State Key Laboratory of Atmospheric Boundary Layer Physics and Atmospheric Chemistry,
21 Institute of Atmospheric Physics, Chinese Academy of Sciences, Beijing, China
22 11 College of Global Change and Earth System Science, Beijing Normal University, Beijing,
23 China
24 12 Multiphase Chemistry Department, Max Planck Institute for Chemistry, Mainz, Germany
25 13 Department of Advanced Technology Fusion, Konkuk University, Seoul, South Korea
26 14 Ministry of Education Key Laboratory for Earth System Modeling, Center for Earth System
27 Science, Tsinghua University, Beijing, China
28 15 Center for Global and Regional Environmental Research, University of Iowa, Iowa City,
29 IA, USA
30 Correspondence to: M. Gao (mmgao2@hkbu.edu.hk), Z. Han (hzw@mail.iap.ac.cn), and G. R.
31 Carmichael (gcarmich@engineering.uiowa.edu)

32
33
34
35
36

37 **Abstract**

38 Topic 3 of the Model Inter-Comparison Study for Asia (MICS-Asia) Phase III examines how
39 online coupled air quality models perform in simulating wintertime haze events in the North
40 China Plain region and evaluates the importance of aerosol radiative and microphysical
41 feedbacks. This paper discusses the estimates of aerosol radiative forcing, aerosol feedbacks,
42 and possible causes for the differences among the participating models. Over the Beijing-
43 Tianjin-Hebei (BTH) region, the ensemble mean of estimated aerosol direct radiative forcing
44 (ADRF) at the top of atmosphere, inside the atmosphere and at the surface are -1.1, 7.7 and -
45 8.8 W/m², respectively. Subdivisions of direct and indirect aerosol radiative forcing confirm
46 the dominant role of direct forcing. During severe haze days (January 17-19, 2010), the
47 averaged reduction in near surface temperature for the BTH region can reach 0.3-1.6 °C. The
48 responses of wind speeds at 10 m (WS10) inferred from different models show consistent
49 declines in eastern China. For the BTH region, aerosol-radiation feedback induced daytime
50 changes in PM_{2.5} concentrations during severe haze days range from 6.0 to 12.9 µg/m³ (< 6%).
51 Sensitivity simulations indicate the important effect of aerosol mixing states on the estimates
52 of ADRF and aerosol feedbacks. Besides, BC exhibits large contribution to atmospheric
53 heating although it accounts for a small share of mass concentration of PM_{2.5}.

54

55 **1 Introduction**

56 Aerosols change weather and climate via the following pathways: they absorb and scatter solar
57 and thermal radiation to alter the radiative balance of the earth-atmosphere system (*Gao et al.*,
58 *2019b*; *Liu et al.*, *2011*; *Jia et al.*, *2018*), which is referred to as direct effects; and, they serve
59 as cloud condensation nuclei (CCN) and/or ice nuclei (IN) to modify cloud properties, which
60 is referred to as indirect effects (*Haywood and Boucher*, *2000*). The suppression of cloud
61 convection induced by direct effects of absorbing aerosols is known as the semi-direct effect
62 (*Huang et al.*, *2006*; *Lohmann and Feichter*, *2005*). Increases in cloud droplet number can
63 increase cloud albedo for a constant liquid water path (LWP), which is further classified as the
64 first indirect effect or Twomey effect (*Twomey*, *1991*). More but smaller cloud droplets reduce
65 precipitation intensity but increase cloud lifetime, which is known as the cloud lifetime or

66 second indirect aerosol effect (*Albrecht, 1989*). In turn, changes in the radiative balance can
67 alter meteorological variables (e.g. temperature, relative humidity, photolysis rate, etc.) and
68 further the transport, diffusion and chemical conversion of trace gases and aerosols, while
69 changes in clouds can affect in-cloud aqueous-phase chemistry and wet deposition of gases and
70 aerosols.

71 The impacts of meteorology on chemistry have been explicitly treated in chemical transport
72 models (CTMs). For example, temperature modulates chemical reaction and photolysis rates,
73 affects volatility of chemical species, and biogenic emissions, wind speed and direction
74 determine transport and mixing, and precipitation influences wet deposition (*Baklanov et al.,*
75 *2014*). However, due to the complexity of these processes and lack of computational resources,
76 the influences of atmospheric compositions on weather and climate have been generally
77 ignored in previous CTMs (*Baklanov et al., 2014*). Studies examining how aerosols interact
78 with weather/climate remain uncertain and limited. Recently, with the rapid development of
79 coupled meteorology and chemistry models, many new studies have been conducted to
80 investigate the aerosol direct and indirect effects and feedbacks (*Baklanov et al., 2017; Forkel*
81 *et al., 2015; Gao et al., 2016, 2017; Grell et al., 2005; Han et al., 2010; Huang et al., 2016;*
82 *Jacobson et al., 2007; Saide et al., 2012; Wang et al., 2014; Yang et al., 2011; Zhang et al.,*
83 *2010*). In highly polluted regions like Asia, aerosol feedbacks can be particularly important
84 (*Gao et al., 2016, 2017*). High concentrations of aerosols would enhance the stability of
85 boundary layer due to reductions in radiation that reach the surface, which in turn can cause
86 further increases in PM_{2.5} concentrations (*Ding et al., 2016; Gao et al., 2016*).

87 Aerosol feedbacks during haze events in China have been explored using multiple online
88 coupled meteorology-chemistry models, including WRF-Chem (the Weather Research
89 Forecasting model coupled with Chemistry, *Chen et al., 2013, 2018; Gao et al., 2016, 2017,*
90 *2019a; Liu et al., 2015*), WRF-CMAQ (Community Multiscale Air Quality, *Wang et al., 2014*).
91 Nevertheless, large uncertainties remain in the modelling of these processes, due to the lack of
92 direct observational constraints and challenges in predicting properties of aerosols. Thus, the
93 inter-comparison of coupled meteorology-chemistry models is of great significance to better
94 understand the differences, causes, and uncertainties within these processes.

95 Topic 3: air quality and climate change within the Model Inter-Comparison Study for Asia

96 Phase III (MICS-Asia phase III) was initialized to address these issues (*Gao et al., 2018a*).
97 Results from seven applications of fully online coupled meteorology-chemistry models using
98 harmonized emission and chemical boundary conditions were submitted to this topic (*Gao et*
99 *al., 2018a*). These model applications include two applications of WRF-Chem by different
100 institutions, two applications of the National Aeronautics and Space Administration (NASA)
101 Unified WRF (NU-WRF) model with different model resolutions, one application of the
102 Regional Integrated Environment Modeling System with Chemistry (RIEMS-Chem, *Han et al.,*
103 *2010*), one application of the coupled Regional Climate Chemistry Modeling System
104 (RegCCMS), and one application of the coupled WRF-CMAQ model (*Gao et al., 2018a*). More
105 detailed information of the participating models, and information about how the experiments
106 were designed and how models perform have been archived in *Gao et al. (2018a)*.

107 In this paper, we analyze the results from the participating models to address the following
108 questions: (1) how large is the aerosol radiative forcing during winter haze in China and how
109 differently are models estimating it? (2) how do aerosol feedbacks change meteorological
110 variables? and how do current models differ in estimating these changes? (3) how do aerosol
111 feedbacks contribute to the evolution of high aerosol concentrations during winter haze
112 episodes? and what are the best estimates from different models? And (4) what are the major
113 causes of the differences among the models? Sect. 2 describes briefly how the experiments
114 were designed and how models perform. Sect. 3 presents the estimates of aerosol direct
115 radiative forcing inferred from multiple models, including the separation of direct and indirect
116 effects. In Sect. 4, we discuss the impacts of aerosol-radiation feedbacks on meteorological
117 variables and PM_{2.5} concentrations. Sect. 5 illustrates the sensitivity of aerosol forcing to
118 different processes in the model, and the summary is presented in Sect. 6.

119

120 **2 Overview of MICS-Asia III Topic 3**

121 The participants were requested to use common emissions to simulate air quality during
122 January 2010 and submit requested model variables. The participating models include one
123 application of the Weather Research Forecasting model coupled with Chemistry (WRF-Chem;
124 Fast et al., 2006; *Grell et al., 2005*) by Pusan National University (PNU) (M1); one application

125 of the WRF-Chem model by the University of Iowa (UIOWA) (M2); two applications (two
126 domains: 45 and 15 km horizontal resolutions) of the National Aeronautics and Space
127 Administration (NASA) Unified WRF (NU-WRF; *Peters-Lidard et al., 2015*) model by the
128 Universities Space Research Association (USRA) and NASA's Goddard Space Flight Center
129 (M3 and M4); one application of the Regional Integrated Environment Modeling System with
130 Chemistry (RIEMS-Chem; *Han et al., 2010*) by the Institute of Atmospheric Physics (IAP),
131 Chinese Academy of Sciences (M5); one application of the coupled Regional Climate
132 Chemistry Modeling System (RegCCMS; *Wang et al., 2010*) from Nanjing University (M6);
133 and one application of the coupled WRF-CMAQ (Community Multiscale Air Quality) model
134 by the University of Tennessee at Knoxville (UTK) (M7) (Table 1). A new Asian emission
135 inventory was developed for MICS-Asia III by integrating state-of-the-art national or regional
136 inventories (*Li et al., 2017*), which was provided to all modeling groups, along with biogenic
137 emissions, biomass burning emissions, etc. Simulations from two global chemical transport
138 models (e.g., GEOS-Chem (The Goddard Earth Observing System Model-Chemistry) and
139 MOZART (Model for OZone And Related chemical Tracers)) were provided as boundary
140 conditions for MICS-Asia III. The entire month of January 2010 was simulated and covered
141 by one single simulation for each participating model. Comprehensive model evaluations
142 indicate that all models could capture the observed near-surface temperature and water vapor
143 mixing ratio, but overestimated near-surface wind speeds. These models were able to represent
144 the observed daily maximum downward shortwave radiation, particularly low values during
145 haze days. The observed variations of air pollutants, including SO₂, NO_x, CO, O₃, PM_{2.5}, and
146 PM₁₀, were reproduced by these models. However, large differences in the models were found
147 in the predicted PM_{2.5} chemical compositions.

148

149 **3 Aerosol Direct and Indirect Forcing**

150 **Fig. 1** shows the monthly mean all-sky aerosol direct radiative forcing (ADRF) over China.
151 The spatial distributions of ADRF at the surface and inside the atmosphere inferred from
152 multiple models are generally consistent, with the largest values in eastern and southwestern
153 China. Over the Beijing-Tianjin-Hebei (BTH) region (areas marked in Figure S1), M7 reports

154 the highest ADRF at the surface (-17.0 W/m^2), and the largest ADRF inside the atmosphere
155 (14.6 W/m^2) (**Table 2**). M6 shows the lowest ADRF both at the surface and inside the
156 atmosphere (-3.6 and 3.6 W/m^2) (**Table 2**). It is noticed that M6 predicts lower aerosol optical
157 depth (AOD) than M7 (*Gao et al., 2018a*), which could partly explain the weaker ADRF
158 estimated by M6. M6 uses an external assumption of aerosol mixing states, which is likely to
159 cause weaker absorption and ADRF in the atmosphere (*Conant et al., 2003*). However, the
160 reported ADRF at the top of the atmosphere (TOA) vary widely, and no consensus is reached
161 on whether the forcing is positive or negative. The spatial pattern of ADRF at the TOA inferred
162 from M5 are consistently negative across the modeling domain, while the results inferred from
163 other models are patchy with positive values to the north or to the southwest (**Fig. 1**). Consistent
164 negative ADRF at the TOA estimated by M5 is related to the strong negative forcing at the
165 surface and the predicted high concentrations of sulfate by M5 (*Gao et al., 2018a*). Over the
166 BTH region, simulated ADRF at the TOA range from -2.6 to 0.2 W/m^2 (**Table 2**). *Li et al.*
167 (*2010*) reported observation-based estimates of aerosol radiative forcing across China to be
168 0.3 ± 1.6 at the TOA. *Chung et al. (2005)* and *Chung et al. (2010)* estimated the forcing over
169 south Asia to be -2.9 W/m^2 and -3.6 W/m^2 at the TOA, respectively. The magnitudes of the
170 model estimated aerosol radiative forcing values are generally in line with these estimates
171 inferred from observations, while discrepancies among models could be due to assumptions of
172 aerosol mixing states and other model treatments (parameterization of hygroscopicity, soil dust,
173 etc.). The discussions on how different model treatments affect the results of ADRF is provided
174 in Sect. 5.

175 **Fig. 2** exhibits the ensemble mean of monthly averaged ADRF at the TOA, inside the
176 atmosphere and at the surface. Elevated forcing inside the atmosphere and at the surface are
177 mainly located in east China. However, the ensemble mean of forcing at the TOA over the
178 ocean is slightly higher than that over the land. Over the BTH region, the ensemble mean of
179 ADRF at the TOA, inside the atmosphere and at the surface are -1.1 , 7.7 and -8.8 W/m^2 ,
180 respectively. In winter, the aerosol radiative forcing in China is largely contributed by the
181 power sector and residential sector, but with different signs of the contribution (*Gao et al.,*
182 *2018b*).

183 M4 and M5 further provide subdivision of direct and indirect aerosol radiative forcing. As

184 listed in **Table 3**, although the magnitudes of forcing estimated by M4 and M5 differ from each
185 other, the dominant roles of direct forcing are consistent. Over North China and during
186 wintertime, aerosol indirect forcing is negligible due to the lack of water vapor and the stable
187 weather conditions.

188

189 **4 Impact of aerosol feedbacks on meteorological variables and PM_{2.5}** 190 **concentrations**

191 When extreme haze events happen, high aerosol loadings can reduce significantly the
192 shortwave radiation reaching the surface, modifying near-surface temperature (*Gao et al.*,
193 2017). **Fig. 3** displays the aerosol-radiation feedback induced changes in temperature at 2 m
194 (T2) from M1 (a), M2 (b), M4 (c), M5 (d), M6 (e), M7 (f) (Table 1: M1: WRF-Chem, Pusan
195 National University; M2: WRF-Chem, University of Iowa; M4: NU-WRF, NASA; M5:
196 RIEMS-Chem, Institute of Atmospheric Physics; M6: RegCCMS, Nanjing University; M7:
197 WRF-CMAQ, University of Tennessee; *Gao et al.*, 2018a). The participating models show
198 different degrees of reductions in T2. M5 exhibits the most widespread areas with reductions,
199 which include Northeastern China. However, significant reductions in T2 inferred from other
200 models are mainly concentrated in southern China (**Fig. 3**). In Beijing (areas marked in Figure
201 S1), the monthly averaged reductions in T2 from multiple models range from 0 to 0.7 °C, with
202 the greatest changes calculated from M4 (**Table 2**). In the Beijing-Tianjin-Hebei (BTH) region,
203 similar magnitudes (0-0.8 °C) are found. When only severe haze days (January 17-19) are
204 considered, the averaged reductions in T2 for Beijing (0.1-1.7 °C) and the BTH region (0.3-1.6
205 °C) are further enhanced (**Table 4**). In terms of aerosol-radiation feedback induced temperature
206 reduction, M1 and M2 generally report similar magnitudes, which are lower than M4, M5 and
207 M7. Model evaluations of PM_{2.5} composition in *Gao et al. (2018a)* reveal that M4 overpredicts
208 the concentrations of organic carbon, which could be one of the reasons for the higher estimated
209 reductions in T2 due to aerosols.

210 Pronounced decreases in water vapor at 2 m (Q2) are mostly located in southern China (**Fig.**
211 **4**), where water vapor is more abundant due to the proximity to the sea. During extreme haze
212 days, the aerosol-radiation feedback induced decreases in Q2 in the BTH region from multiple

213 models range from 0.07 to 0.29 g/kg, with the lowest estimate from M1 and the highest from
214 M4 (**Table 4**).

215 The responses of wind speeds at 10 m (WS10) inferred from different models are generally
216 consistent, displaying decreases in eastern China except M6 (**Fig. 5**). In the BTH region, the
217 monthly mean aerosol-radiation feedback induced decreases in WS10 range from 0.02 to 0.09
218 m/s (**Table 2**), and more pronounced reductions are suggested by M4 and M7 (**Fig. 5**).

219 Because of aerosol-radiation feedback, most models report that surface PM_{2.5} concentrations
220 are enhanced in China, with the exception of M6 (**Fig. 6**). It is also noteworthy that PM_{2.5}
221 concentrations decrease in the Gobi desert and Taklimakan desert of western China in M5 and
222 M2, which is caused by the decreased wind speed near the surface due to the weakened
223 downward transport of momentum from upper layer above boundary layer to the surface (*Han*
224 *et al.*, 2013). The changes of PM_{2.5} concentrations suggested by M6 are patchy over east China,
225 with decreases to the north and to the southwest. The monthly mean PM_{2.5} are enhanced by 0.1-
226 1.6 $\mu\text{g}/\text{m}^3$ for Beijing, and by 0.8-2.2 $\mu\text{g}/\text{m}^3$ for the BTH region. The enhancement fractions
227 are generally below 2% for Beijing, and below 4% for the BTH region (**Table 2**).

228 To further understand how aerosol-radiation feedback contributes to the formation of haze
229 event, we calculate the mean increase during extreme haze days (January 17-19). For the BTH
230 region, the contribution of aerosol-radiation feedback to PM_{2.5} concentrations are lower than
231 4%, and the enhancement are below 8.5 $\mu\text{g}/\text{m}^3$. *Gao et al.* (2017) demonstrates that the aerosol-
232 radiation feedback induced changes in PM_{2.5} are negligible during nighttime, so we further
233 calculate daytime mean changes, as listed in **Table 4**. For the BTH region, M2 reports the
234 largest enhancement (12.9 $\mu\text{g}/\text{m}^3$) of PM_{2.5} concentrations during daytime. Other models,
235 except M6, report similar magnitudes of enhancement, ranging from 5.3 to 6.6 $\mu\text{g}/\text{m}^3$. The
236 enhancement fraction remains less than 6% for the BTH region, and below 8.3% for Beijing.
237 **Table 4** also displays the maximum enhancement of PM_{2.5} during haze days over the BTH
238 region. M7 suggests the largest PM_{2.5} enhancement (up to 60.9 $\mu\text{g}/\text{m}^3$), followed by M2 (up to
239 55.4 $\mu\text{g}/\text{m}^3$). Other three models, M1, M4, M5, and M6 indicate the aerosol-radiation induced
240 increase in PM_{2.5} can reach up to more than 20 $\mu\text{g}/\text{m}^3$ in the BTH region (**Table 4**).

241 The contributions of aerosol-radiation feedback to haze formation in China have been
242 investigated in many previous studies (*Ding et al.*, 2016; *Gao et al.*, 2015; *Gao et al.*, 2016;

243 *Liu et al., 2018; J. Wang et al., 2014; Z. Wang et al., 2014; Wang et al., 2015; Wu et al., 2019;*
244 *Zhang et al., 2015; Zhang et al., 2018; Zhong et al., 2018*), but the reported values diverge.
245 *Ding et al. (2016), J. Wang et al. (2014) and Zhong et al. (2018)* indicate that the aerosol
246 radiative effects can increase PM_{2.5} by more than 100 µg/m³ or +70%. *Gao et al. (2015), Z.*
247 *Wang et al. (2014), Wang et al. (2015), and Zhang et al. (2018)* suggest that the contributions
248 are generally within the range of 10-30%. These reports are different from this study in terms
249 of study periods, region, and pollution levels. Most of previous reports focused on the January
250 2013 haze episodes (*J. Wang et al., 2014*), while the monthly mean concentrations of PM_{2.5} in
251 January 2010 are nearly 50% lower than that of January 2013. According to the findings in this
252 study, the contribution of aerosol-radiation feedback to haze formation during January 2010
253 are generally below 10%. Uncertainties still remain as suggested by the errors in the simulated
254 chemical compositions (*Gao et al., 2018a*). Concentrations of sulfate and organic aerosol are
255 generally underestimated by most of the participating models, and M4 overestimates the
256 concentrations of organic aerosols (*Gao et al., 2018a*). These model errors were attributed to
257 the missing multiphase oxidation mechanisms of sulfate, and different treatments of secondary
258 organic aerosol (SOA) formation in these models (*Gao et al., 2018a*).

259

260 **5 Sensitivity to Different Processes**

261 To explore the potential causes for the differences among models, and the major factors that
262 influence aerosol-radiation feedback, several sensitivity simulations were conducted with the
263 RIEMS-Chem model (M5) (*Han et al., 2010*). These simulations aim to examine the effects of
264 mixing states of aerosols, hygroscopic growth, black carbon and soil dust.

265 5.1 Aerosol mixing states

266 In the control simulation, inorganic aerosols and BC are assumed to be internally mixed to form
267 a homogeneous mixture. The refractive index of this mixture is estimated using the volume-
268 weighted average of the refractive index of individual component. The size of the mixture is
269 prescribed to be the maximum size of the mixed aerosol components. For example, the size of
270 the mixture of sulfate and BC is set to be equal to the size of sulfate, assuming a small BC
271 particle sticking to a larger sulfate particle.

272 An additional simulation was conducted with the aerosols were treated as externally mixed,
273 and the corresponding results are displayed in **Fig. 7-9**. For external mixing assumption, each
274 aerosol component is considered individually, and the total AOD is calculated as the sum of
275 extinction by each aerosol component. Compared with the results with internal mixing
276 assumption, results with external mixing assumption generally exhibit a weaker (negative)
277 ADRF at the surface (~15%), a stronger (negative) ADRF at TOA (~50%) and a decreased
278 (positive) ADRF in the atmosphere (~30%) (**Fig. 9a, 9f, 9k**). These responses of ADRF to the
279 assumption of aerosol mixing states are consistent with *Conant et al. (2003)*. However, *Curci*
280 *et al. (2015)* reported lower AOD with internal mixing assumption than with external mixing
281 assumption. In *Curci et al. (2015)*, aerosol mass was distributed in less numerous particles with
282 larger sizes. As a result, fewer scattering agents and lower AOD were estimated.

283 Aerosol feedbacks estimated by M5 also tend to be weaker with external mixing assumption
284 than with internal mixing assumption (changes in surface meteorological variables and PM_{2.5}
285 concentrations, **Fig. 8a, 8d, 8g, and 8j**). The monthly averaged changes in T2, WS10 and PM_{2.5}
286 are -0.6 °C, -0.04 m/s and 2.2 µg/m³ for the BTH region with internal mixing assumption, while
287 the corresponding values change to -0.6 °C, -0.03 m/s and 1.8 µg/m³ with external mixing
288 assumption. These differences emphasize the important influences of aerosol mixing states on
289 the estimates of ADRF and aerosol feedbacks. However, aerosol mixing states are also varying
290 with time and location. Measurements in North China suggest that aerosols are partially
291 internally mixed, and the fraction of internal mixing increased from clean to haze periods (*Li*
292 *et al., 2014*).

293 294 5.2 Hygroscopic growth

295 Given the appreciable effect of aerosol hygroscopic growth on ADRF (*Li et al., 2014*), another
296 simulation was conducted with decreased relative humidity (RH). In this simulation, FNL
297 nudging was applied above boundary layer to reduce RH This perturbation of RH was based
298 on the fact that M5 overestimates relative humidity (water vapor mixing ratio) (*Gao et al.,*
299 *2017*). With reduced RH, lower values of AOD (**Fig. 7f**) and weaker ADRF at the surface and
300 TOA (**Fig. 9e, 9j, and 9o**, about 15% lower) are found, mainly because of suppressed
301 hygroscopic growth under lower relative humidity.

302

303 5.3 Soil dust and sea salt

304 M5 (RIEMS-Chem) includes naturally emitted soil dust and sea salt, while the other models
305 except M2 (WRF-Chem, University of Iowa) do not consider soil dust in their model settings.
306 In an additional sensitivity simulation, soil dust and sea salt emissions were turned off in M5
307 to examine the influence on ADRF and aerosol feedbacks (**Fig. 9d, 9l and 9n**). In January 2010,
308 significant amounts of soil dust were emitted from the Taklimakan desert, influencing wide
309 areas of China. M5 estimates that the monthly mean ADRF at the surface due to dust and sea
310 salt is about -12 W/m^2 over the Taklimakan desert, $-4\sim-6 \text{ W/m}^2$ in the middle reaches of the
311 Yellow River and the Yangtze River Delta, and about $-2\sim-4 \text{ W/m}^2$ over the BTH region. Over
312 the BTH region, the contribution of dust and sea salt aerosols to total ADRF can reach 5~10%.
313 Table 2 illustrates that M5 predicts the largest (negative) radiative forcing at TOA over the BTH
314 region. The above analyses with reduced relative humidity and perturbations in dust and sea
315 salt suggest that the inclusion of dust and overprediction of relative humidity by M5 are
316 important reasons.

317

318 5.4 The effect of BC

319 Two sets of simulations, namely without BC and with doubled BC concentrations, were
320 conducted to examine the influences of BC on aerosol radiative forcing and feedbacks. In the
321 control simulation, the aerosol induced changes in monthly T2, WS10 and PM_{2.5} are $-0.6 \text{ }^\circ\text{C}$, $-$
322 0.04 m/s and $2.2 \text{ } \mu\text{g/m}^3$ for the BTH region, respectively. When BC is not included (only
323 scattering aerosols and dust), the corresponding aerosol induced changes are $-0.5 \text{ }^\circ\text{C}$, -0.02 m/s
324 and $1.0 \text{ } \mu\text{g/m}^3$, respectively. When BC concentrations are doubled, these values change to -0.7
325 $^\circ\text{C}$, -0.05 m/s and $3.2 \text{ } \mu\text{g/m}^3$, respectively. The comparison between the control case and two
326 additional sensitivity cases indicates that the changes caused by BC are comparable to those by
327 scattering aerosols. The contribution of BC to aerosol feedbacks can reach up to 40~50%. It is
328 also found that the influence of BC on aerosol feedbacks with internal mixing assumption is
329 larger than that with external mixing assumption (Figure not shown).

330 Large uncertainties still remain in the estimates of the role of BC in aerosol feedbacks relative
331 to scattering aerosols. *Gao et al. (2016)* suggested that the impacts of BC on boundary layer

332 height and PM_{2.5} concentrations can account for as high as 60% of the total aerosol feedbacks
333 in the North China Plain at 2 p.m., although it only accounts for a small share of PM in terms
334 of mass concentration. *Qiu et al. (2017)* indicated that PM_{2.5} concentrations averaged over the
335 North China Plain increased by 16.8% and 1.0% due to scattering aerosols and BC, respectively.
336 It should be noted that most participating models, including RIEMS-Chem, tend to
337 underpredict the total mass concentrations of scattering aerosols (inorganic and organic
338 aerosols) by up to a factor of two over the study period, leading to overestimation of the
339 contribution of BC.

340

341 **6 Summary**

342 Topic 3 of MICS-Asia III (*Gao et al., 2018a*) focuses on understanding how current online
343 coupled air quality models perform in capturing extreme aerosol pollution event in North China
344 and how aerosols interact with radiation and weather. Seven applications of different online
345 coupled meteorology-chemistry models were involved in this activity. *Gao et al. (2018a)* has
346 demonstrated that main features of the accumulation of air pollutants are generally well
347 represented, while large differences in the models were found in the predicted PM_{2.5} chemical
348 compositions. These inconsistencies would lead to differences in estimated ADRF and aerosol
349 feedbacks.

350 The spatial distributions of ADRF at the surface and inside the atmosphere inferred from
351 multiple models are generally consistent, but the spatial distributions of ADRF at the TOA
352 estimated by these models greatly differ. Over the BTH region, the ensemble mean of ADRF
353 at the TOA, inside the atmosphere and at the surface are -1.1, 7.7 and -8.8 W/m², respectively.
354 Subdivisions of direct and indirect aerosol radiative forcing confirm the dominant roles of
355 direct forcing.

356 During severe haze days (January 17-19), the averaged reduction in T₂ for the BTH region can
357 reach 0.3-1.6 °C. The responses of wind speeds at 10 m (WS₁₀) inferred from different models
358 show consistent declines in eastern China. For the BTH region, aerosol-radiation feedback
359 induced changes in daytime PM_{2.5} range from 5.3 to 12.9 µg/m³ (< 6%). Our findings differ
360 from previous studies (*Ding et al., 2016; Gao et al., 2015; Gao et al., 2016; Liu et al., 2018;*

361 *J. Wang et al., 2014; Z. Wang et al., 2014; Wang et al., 2015; Wu et al., 2019; Zhang et al.,*
362 *2015; Zhang et al., 2018; Zhong et al., 2018)* in terms of study period, region and pollution
363 levels. The monthly mean concentrations of PM_{2.5} in January 2010 (current study period)
364 are about 50% lower than those in January 2013.

365 Sensitivity simulations were conducted with the RIEMS-Chem model (M5) to understand the
366 influences of aerosols mixing states, hygroscopic growth, black carbon and soil dust. The
367 results indicate the important effect of aerosol mixing states on the estimates of ADRF and
368 aerosol feedbacks. It was also found that BC exhibits large contribution to atmospheric heating,
369 but uncertainties remain in estimating its contribution given the fact that the observed aerosol
370 chemical components were not perfectly simulated. *Huang et al. (2015)* separated the
371 contributions of different aerosol components to aerosol direct radiative forcing, highlighting
372 the roles of BC and sulfate. Future studies are also needed to separate the effects of other
373 aerosol components, including sulfate, on aerosol feedbacks.

374

375 **Author Contributions**

376 M.G., Z.H., and G.R.C. designed the study, and M.G. processed and analyzed the data. M.G.,
377 Z.H., and G.R.C. wrote the paper with inputs from all other authors.

378

379 **Data availability**

380 The measurements and model simulations data can be accessed through contacting the
381 corresponding authors.

382

383 **Competing interests**

384 The authors declare that they have no conflict of interests.

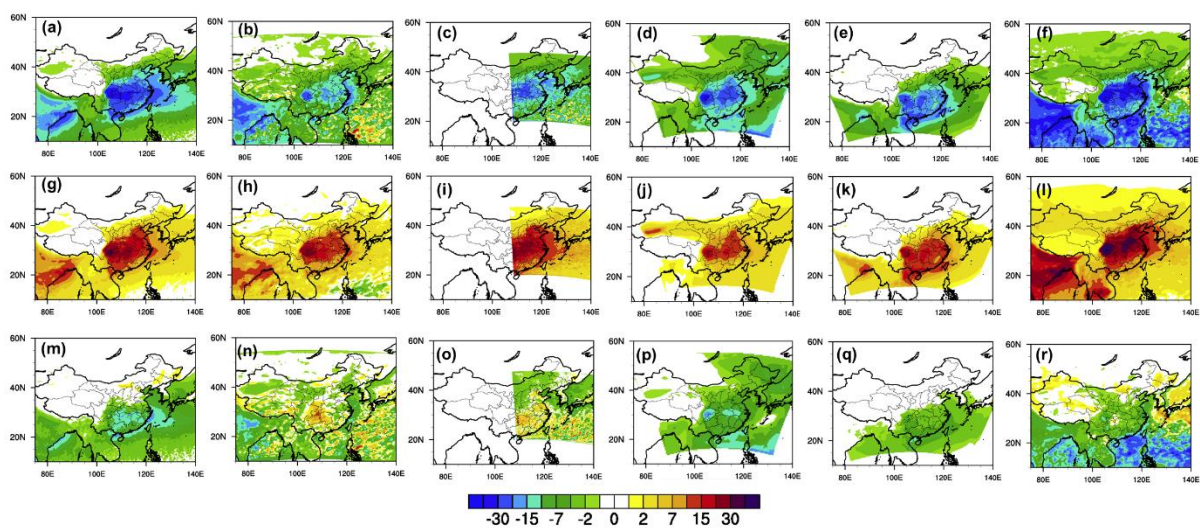
385

386 **Acknowledgement**

387 The authors would like to acknowledge support for this project from the National Natural
388 Science Foundation of China (91644217 and 41620104008).

389

390

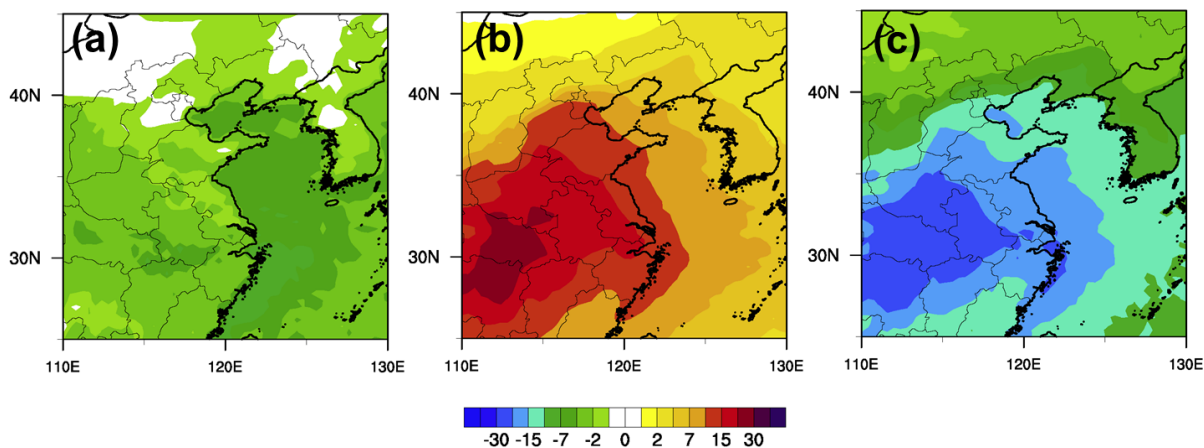


391

392 Figure 1. Monthly (January 2010) mean aerosol direct radiative forcing at the surface, inside the atmosphere and
 393 at the top of the atmosphere inferred from M1 (a, g, m), M2 (b, h, n), M4 (c, i, o), M5 (d, j, p), M6 (e, k, q), M7
 394 (f, l, r) (M1: WRF-Chem, Pusan National University; M2: WRF-Chem, University of Iowa; M4: NU-WRF,
 395 NASA; M5: RIEMS-Chem, Institute of Atmospheric Physics; M6: RegCCMS, Nanjing University; M7: WRF-
 396 CMAQ, University of Tennessee; *Gao et al., 2018a*)

397

398



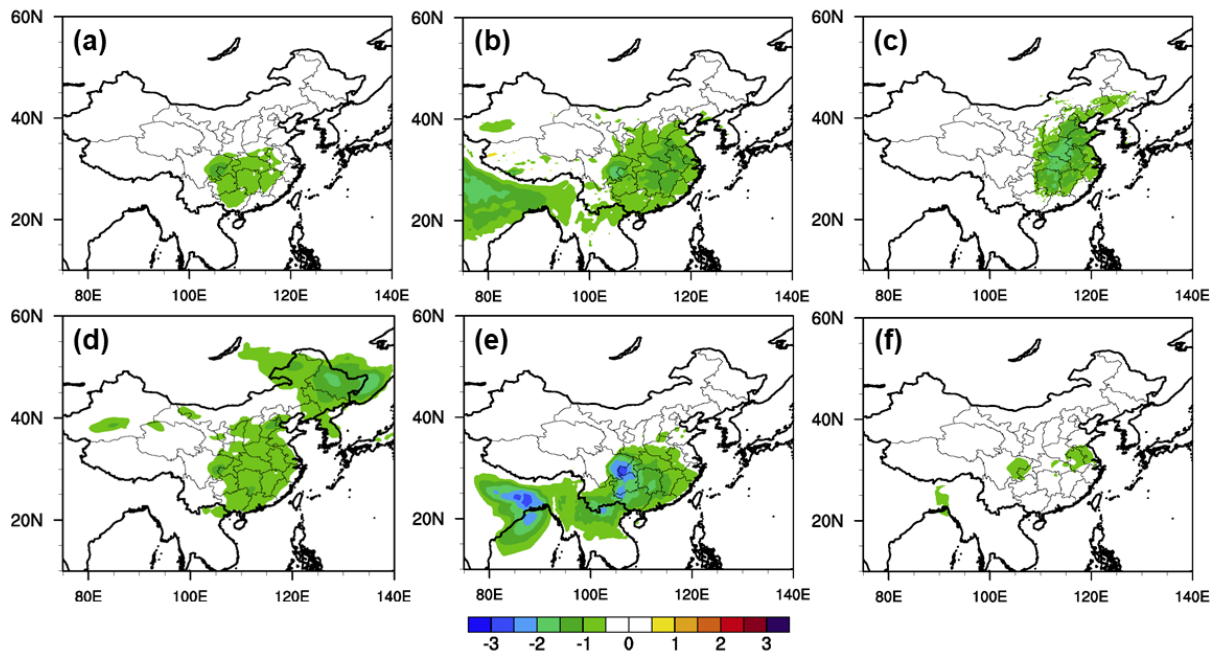
399

400 Figure 2. Ensemble mean of monthly (January 2010) mean aerosol direct radiative forcing at the top of the
 401 atmosphere (a), inside the atmosphere (b) and at the surface (c)

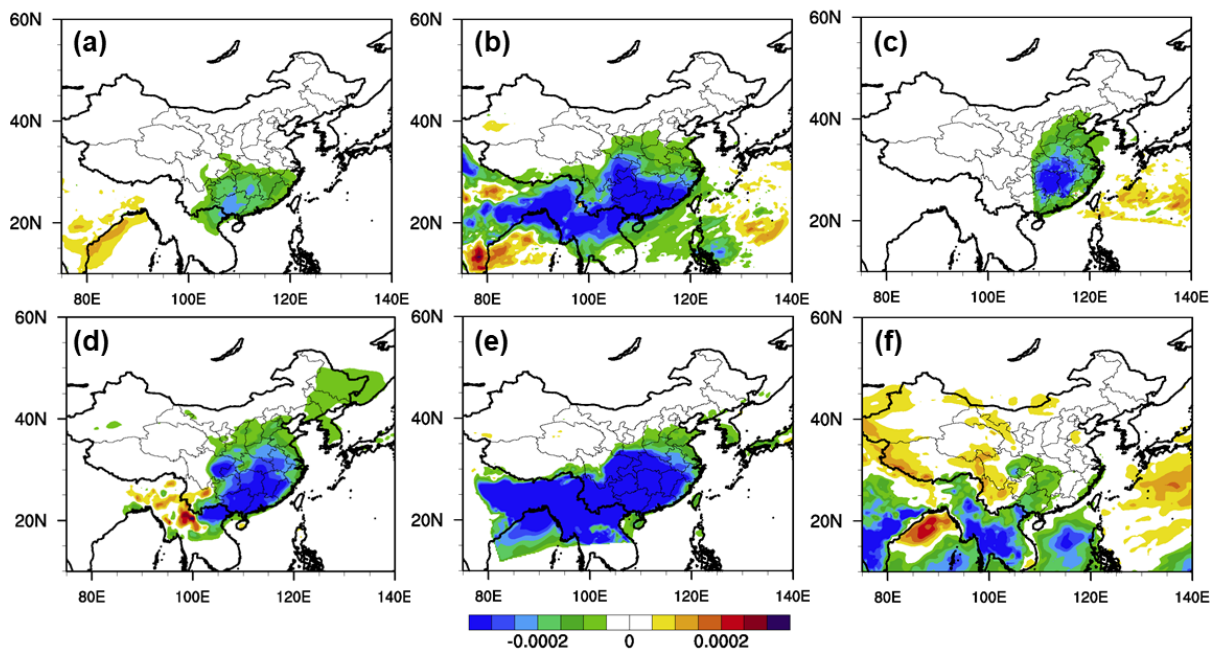
402

403

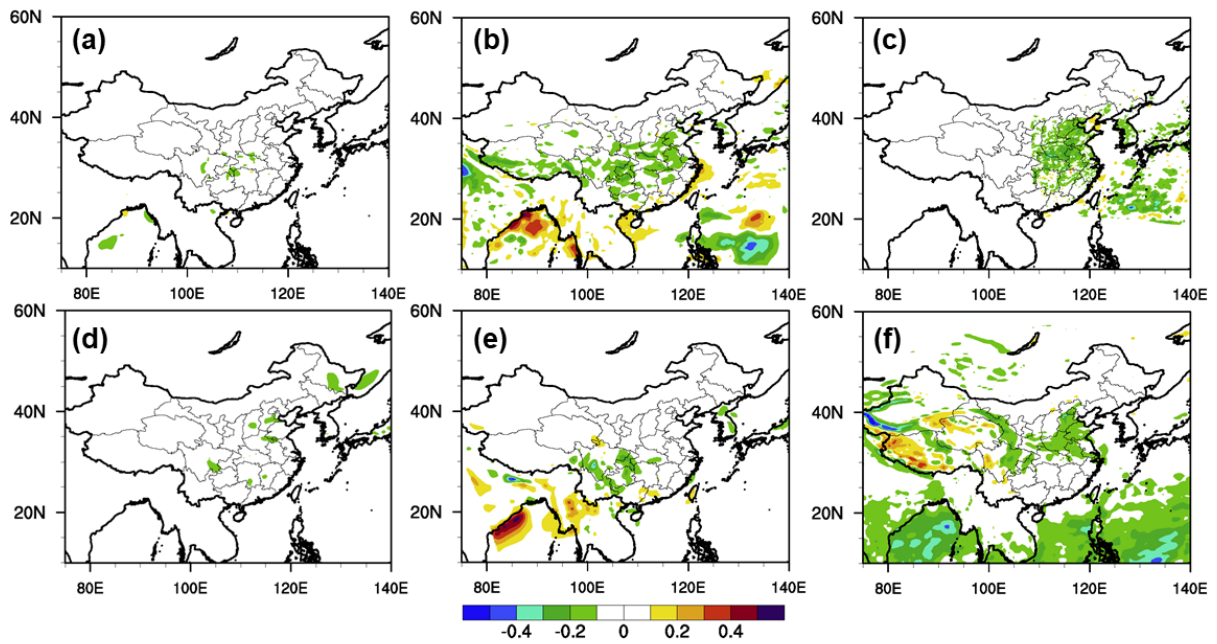
404



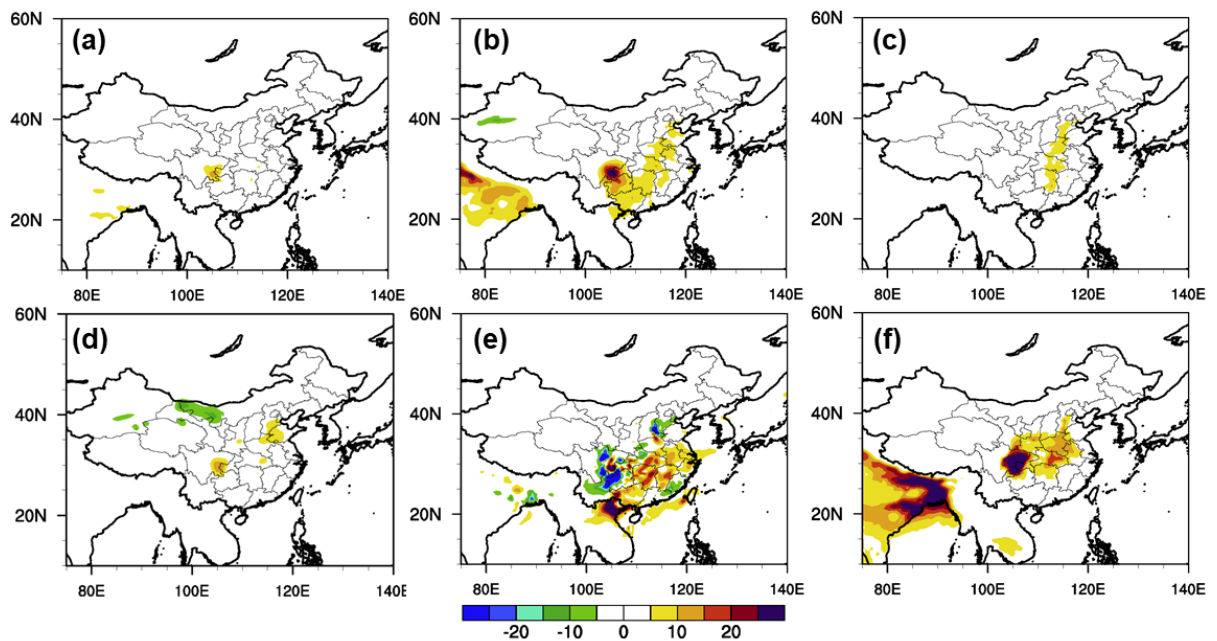
405
 406 Figure 3. Monthly (January 2010) mean changes in temperature at 2 m (T_2 , °C) due to aerosol radiative effects
 407 from M1 (a), M2 (b), M4 (c), M5 (d), M6 (e), M7 (f) (M1: Pusan National University; M2: University of Iowa;
 408 M4: NASA; M5: Institute of Atmospheric Physics; M6: Nanjing University; M7: University of Tennessee; *Gao*
 409 *et al.*, 2018a)
 410



411
 412 Figure 4. Monthly (January 2010) mean changes in water vapor at 2 m (Q_2 , kg/kg) due to aerosol radiative
 413 effects from M1 (a), M2 (b), M4 (c), M5 (d), M6 (e), M7 (f) (M1: Pusan National University; M2: University of
 414 Iowa; M4: NASA; M5: Institute of Atmospheric Physics; M6: Nanjing University; M7: University of
 415 Tennessee; *Gao et al.*, 2018a)
 416

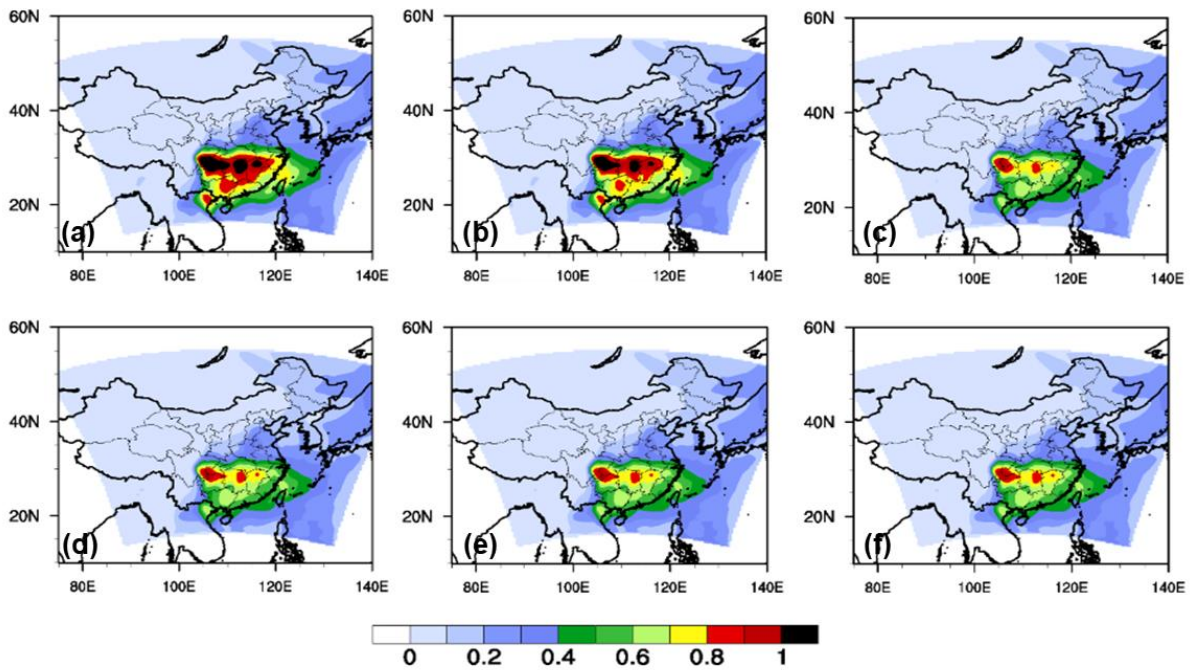


417
 418 Figure 5. Monthly (January 2010) mean changes in wind speeds at 10 m (WS10, m/s) due to aerosol radiative
 419 effects from M1 (a), M2 (b), M4 (c), M5 (d), M6 (e), M7 (f) (M1: Pusan National University; M2: University of
 420 Iowa; M4: NASA; M5: Institute of Atmospheric Physics; M6: Nanjing University; M7: University of
 421 Tennessee; *Gao et al., 2018a*)
 422



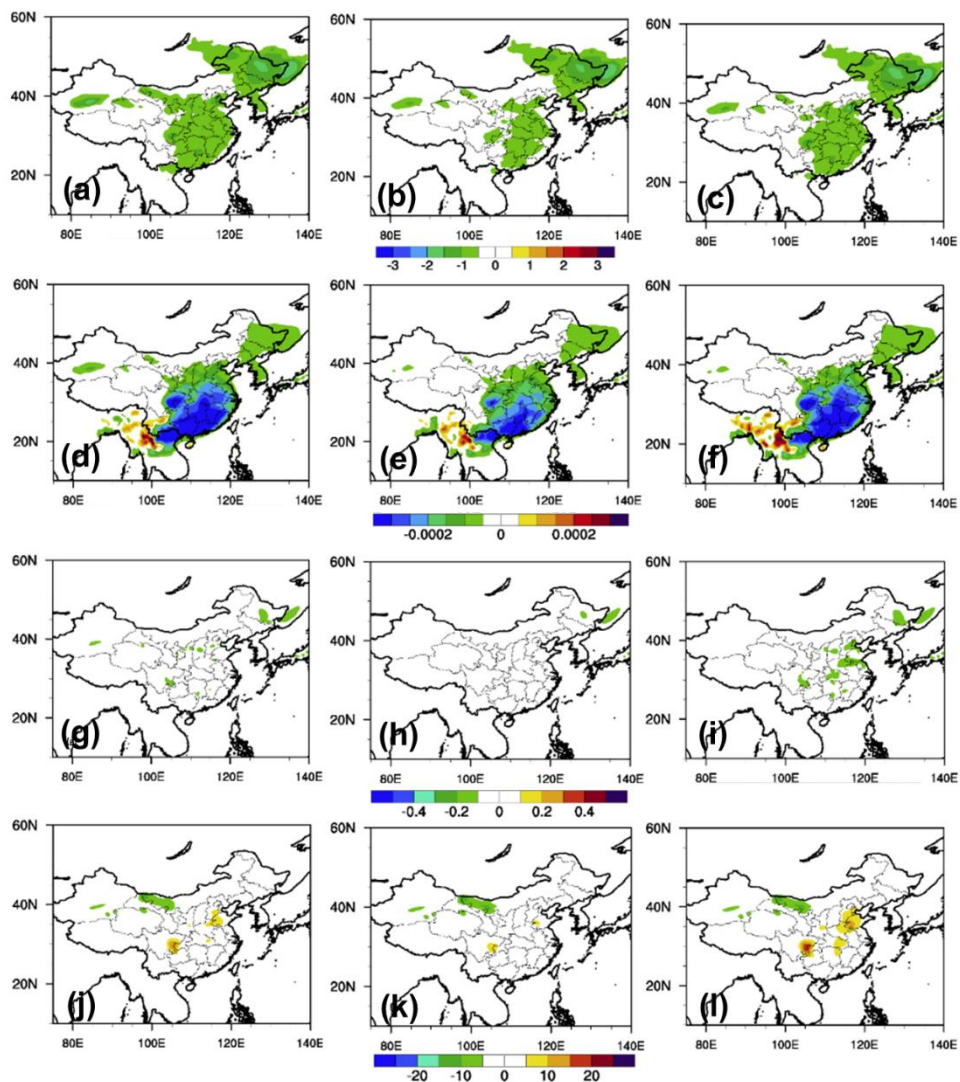
423
 424 Figure 6. Monthly (January 2010) mean changes in surface PM_{2.5} ($\mu\text{g}/\text{m}^3$) due to aerosol radiative effects from
 425 M1 (a), M2 (b), M4 (c), M5 (d), M6 (e), M7 (f) (M1: Pusan National University; M2: University of Iowa;
 426 NASA; M5: Institute of Atmospheric Physics; M6: Nanjing University; M7: University of Tennessee; *Gao et*
 427 *al., 2018a*)
 428

429
430



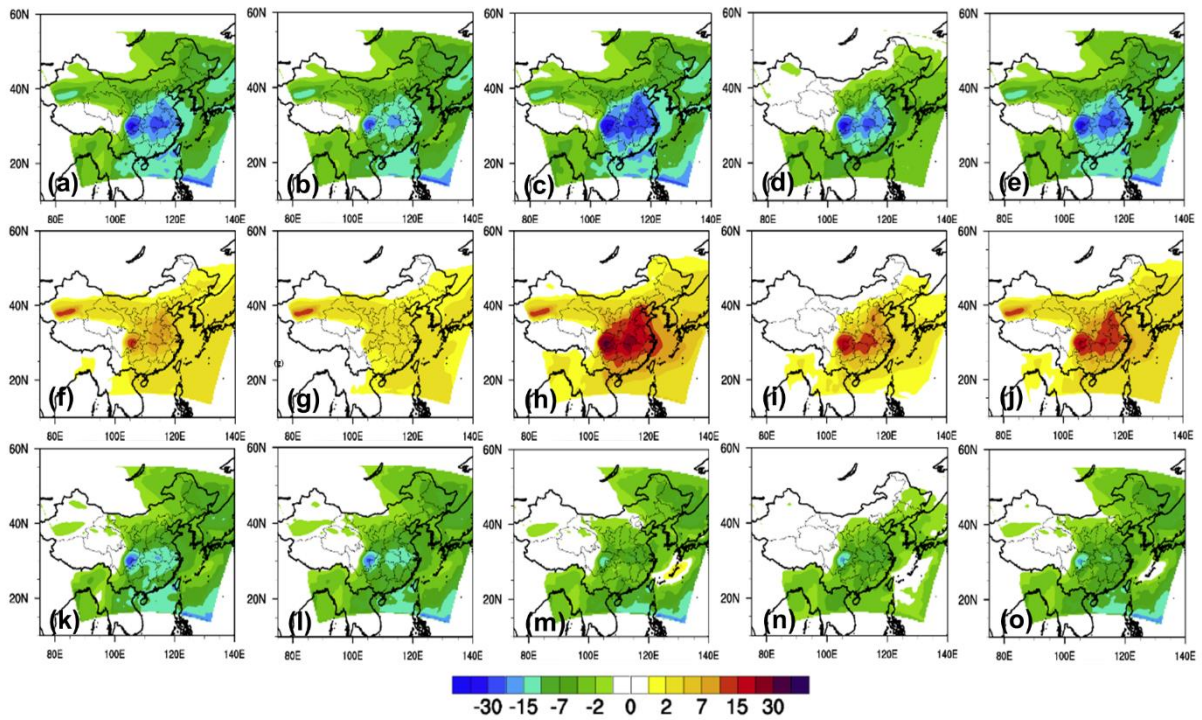
431
432
433
434
435
436
437

Figure 7. Monthly (January 2010) mean RIEMS-Chem modeled AOD from different simulations: control run (default simulation with internal mixing assumption) (a), external mixing assumption (b), internal mixing assumption but without BC (c), internal mixing assumption but with doubled BC (d), without dust and sea-salt (e), and reduced RH (f)



438
 439
 440
 441
 442
 443
 444

Figure 8. Monthly (January 2010) mean RIEMS-Chem modeled changes in T2 (°C), Q2 (kg/kg), WS10 (m/s) and PM_{2.5} (µg/m³) from different simulations: external mixing assumption (first column), internal mixing assumption but without BC (second column) and internal mixing assumption but with doubled BC (third column)



445

446

Figure 9. Monthly (January 2010) mean RIEMS-Chem modeled aerosol direct radiative forcing at the surface (a-e), inside the atmosphere (f-j) and at the top of the atmosphere (k-o) from different simulations: external mixing assumption (first column), internal mixing assumption but without BC (second column), internal mixing assumption but with doubled BC (third column), without dust and sea-salt (fourth column), and reduced RH (fifth column)

447

448

449

450

451

452

453

454

455

456

457

458

459

460

461

462

463

464

465

466

467

468

469

470
471
472
473

Table 1 Participating models in Topic 3

Models	M1: WRF- Chem1	M2: WRF- Chem2	M3: NU- WRF1	M4: NU- WRF2	M5: RIEMS- Chem	M6: RegCCMS	M7: WRF- CMAQ
Modelling Group	Pusan National University	University of Iowa	USRA/NAS A	USRA/NASA	Institute of Atmospheric Physics	Nanjing University	University of Tennessee
Grid Resolution	45km	50km	45km	15km	60km	50km	45km
Vertical Layers	40 layers to 50mb	27 layers to 50mb	60 layers to 20mb	60 layers to 20mb	16 layers to 100mb	18 layers to 50mb	
Gas phase chemistry	RACM	CBMZ	RADM2	RADM2	CBM4	CBM4	SAPRC99
Aerosols	MADE	MOSAIC- 8bin	GOCART	GOCART	Sulfate, nitrate, ammonium, BC, OC, SOA, 5 bins of soil dust, and 5 bins of sea salt	Sulfate, nitrate, ammonium, BC and POC	AE06
Chemical Boundary Conditions	Climatologica l data from NALROM	MOZART	MOZART GOCART	MOZART GOCART	GEOS-Chem	Climatological data	GEOS- Chem

474
475
476
477
478
479
480
481
482
483
484
485
486
487
488
489
490
491
492
493

494 Table 2 Monthly Mean (January 2010) Aerosol Direct Radiative Forcing (W/m^2) and
 495 Changes in T2 ($^{\circ}C$), Q2 (g/kg), WS10 (0.1 m/s), and PM_{2.5} ($\mu g/m^3$) for Beijing and Beijing-
 496 Tianjin-Hebei region (areas marked in Fig. S1)

Beijing	M1 PNU	M2 UIOWA	M4 NASA	M5 IAP	M6 NJU	M7 UTK
ADRF TOA	-0.6	-2.2	-0.8	-1.4	-0.1	-2.5
ADRF ATM	5.8	4.3	9.3	5.1	2.4	11.6
ADRF SFC	-6.4	-6.5	-10.1	-6.5	-2.5	-14.1
T2	-0.1	-0.3	-0.7	-0.5	-0.1	0.0
Q2	-1.2E-2	-2.3E-2	-6.4E-2	-5.8E-2	-5.8E-3	2.1E-2
WS10	-0.2	-0.2	-0.6	-0.2	0.0	-1.2
PM _{2.5}	0.1 (0.2%)	1.4 (1.6%)	1.1 (1.7%)	0.6 (1.4%)	-1.2 (- 2.2%)	1.0 (1.4%)
BTH						
ADRF TOA	0.2	-1.4	-0.3	-2.6	0.0	-2.4
ADRF ATM	7.3	5.4	10.1	6.3	3.6	14.6
ADRF SFC	-7.1	-6.8	-10.4	-8.9	-3.6	-17.0
T2	-0.2	-0.4	-0.8	-0.6	-0.2	0.0
Q2	-1.0E-2	-2.5E-2	-8.1E-2	-7.6E-2	-2.9E-2	2.5E-2
WS10	-0.2	-0.2	-0.9	-0.4	0.1	-0.9
PM _{2.5}	0.8 (1.4%)	1.8 (1.8%)	2.2 (3.2 %)	2.2 (3.9%)	-4.2 (- 5.7%)	2.2 (2.4%)

497
 498
 499
 500
 501
 502
 503
 504
 505
 506
 507
 508
 509
 510
 511
 512

513 Table 3 Monthly Mean (January 2010) Aerosol Direct Radiative Forcing and indirect
 514 Radiative Forcing (W/m^2) at the top of the atmosphere inferred from M4 and M5 (areas
 515 marked in Fig. S1)

Beijing	direct	Indirect
M4	-0.77	-0.15
M5	-1.43	-0.01
BTH		
M4	-0.28	0.1
M5	-2.63	-0.04

516
 517
 518
 519
 520
 521
 522
 523
 524
 525
 526
 527
 528
 529
 530
 531
 532
 533
 534
 535
 536
 537
 538
 539
 540
 541
 542
 543
 544
 545
 546
 547
 548
 549
 550

551 Table 4 Mean Aerosol (January 2010) Direct Radiative Forcing (W/m^2) and Changes in T2
 552 ($^{\circ}C$), Q2 (g/kg), WS10 (0.1 m/s), and PM_{2.5} ($\mu g/m^3$) for Beijing and Beijing-Tianjin-Hebei
 553 (BTH) region averaged over January 17-19 2010 (areas marked in Fig. S1)

Beijing	M1 PNU	M2 UIOWA	M4 NASA	M5 IAP	M6 NJU	M7 UTK
ADRF TOA	2.6	-1.4	1.8	-3.0	-0.6	-3.3
ADRF ATM	18.6	9.8	21.5	13.3	7.3	32.3
ADRF SFC	-16.0	-11.2	-19.7	-16.3	-7.9	-35.6
T2	-0.5	-0.5	-1.7	-1.3	-0.1	-1.5
Q2	-7.4E-2	-6.2E-2	-2.6E-1	-1.8E-1	-1.3E-2	-9.2E-2
WS10	-0.1	0.2	-2.3	0.4	0.5	-0.8
PM _{2.5}	-1.1 (- 0.9%)	3.8 (1.7%)	6.3 (3.8%)	1.0 (0.8%)	-7.9 (- 4.7%)	1.3 (1.1%)
BTH						
ADRF TOA	1.4	0.1	4.9	-4.6	-0.7	-3.8
ADRF ATM	18.3	12.0	19.1	13.2	10.0	36.1
ADRF SFC	-16.9	-11.9	-14.2	-17.8	-10.7	-39.9
T2	-0.6	-0.7	-1.6	-1.2	-0.3	-1.5
Q2	-7.1E-2	-8.2E-2	-2.9E-1	-2.0E-1	-1.2E-1	-8.9E-2
WS10	-0.3	-0.4	-2.5	0.0	0.3	-0.9
PM _{2.5}	2.9 (2.3%)	8.5 (3.7%)	5.3 (3.9%)	5.3 (3.9%)	-10.5 (- 6.2%)	5.1 (2.7%)
Daytime PM_{2.5}						
Beijing	2.4 (2.0%)	8.5 (3.9%)	8.4 (5.5%)	-0.7 (- 0.6%)	-4.2 (- 3.2%)	10.7 (8.3%)
BTH	6.0 (4.9%)	12.9 (5.9%)	6.6 (5.2%)	5.3 (4.0%)	-6.2 (- 3.8%)	6.4 (3.8%)
	Up to 26.4	Up to 55.4	Up to 26.5	Up to 21.1	Up to 22.8	Up to 60.9

554

555

556

557

558

559

560 **References:**

- 561 Albrecht, B.A.: Aerosols, cloud microphysics, and fractional cloudiness, *Science*, 245(4923),
562 pp.1227-1230, <https://doi.org/10.1126/science.245.4923.1227>, 1989.
- 563 Haywood, J., and Boucher, O.: Estimates of the direct and indirect radiative forcing due to
564 tropospheric aerosols: A review, *Rev. geophys.*, 38(4), pp.513-543,
565 <https://doi.org/10.1029/1999rg000078>, 2000.
- 566 Baklanov, A., Schlünzen, K., Suppan, P., Baldasano, J., Brunner, D., Aksoyoglu, S.,
567 Carmichael, G., Douros, J., Flemming, J., Forkel, R. and Galmarini, S.: Online coupled
568 regional meteorology chemistry models in Europe: current status and prospects, *Atmos.*
569 *Chem. Phys.*, 14(1), pp.317-398, <https://doi.org/10.5194/acpd-13-12541-2013>, 2014.
- 570 Baklanov, A., Brunner, D., Carmichael, G., Flemming, J., Freitas, S., Gauss, M., Hov, Ø.,
571 Mathur, R., Schlünzen, K.H., Seigneur, C. and Vogel, B.: Key Issues for Seamless
572 Integrated Chemistry–Meteorology Modeling, *Bull. Amer. Meteor. Soc.*, 98(11), pp.2285-
573 2292, <https://doi.org/10.1175/bams-d-15-00166.1>, 2017.
- 574 Chen, S., Huang, J., Zhao, C., Qian, Y., Leung, L.R. and Yang, B.: Modeling the transport and
575 radiative forcing of Taklimakan dust over the Tibetan Plateau: A case study in the summer
576 of 2006, *Jour. Geophys. Res.: Atmos.*, 118(2), pp.797-812,
577 <https://doi.org/10.1002/jgrd.50122>, 2013.
- 578 Chen, S., Yuan, T., Zhang, X., Zhang, G., Feng, T., Zhao, D., Zang, Z., Liao, S., Ma, X., Jiang,
579 N. and Zhang, J.: Dust modeling over East Asia during the summer of 2010 using the
580 WRF-Chem model, *Jour. Quant. Spec. Rad. Tran.*, 213, pp.1-12,
581 <https://doi.org/10.1016/j.jqsrt.2018.04.013>, 2018.
- 582 Chung, C.E., Ramanathan, V., Kim, D. and Podgorny, I.A.: Global anthropogenic aerosol
583 direct forcing derived from satellite and ground-based observations, *Jour. Geophys. Res.:*
584 *Atmos.*, 110(D24), <https://doi.org/10.1029/2005jd006356>, 2005.
- 585 Chung, C.E., Ramanathan, V., Carmichael, G., Kulkarni, S., Tang, Y., Adhikary, B., Leung,
586 L.R. and Qian, Y.: Anthropogenic aerosol radiative forcing in Asia derived from regional
587 models with atmospheric and aerosol data assimilation, *Atmos. Chem. Phys.*, 10(13),
588 pp.6007-6024, <https://doi.org/10.5194/acpd-10-821-2010>, 2010.
- 589 Conant, W.C., Seinfeld, J.H., Wang, J., Carmichael, G.R., Tang, Y., Uno, I., Flatau, P.J.,
590 Markowicz, K.M. and Quinn, P.K.: A model for the radiative forcing during ACE - Asia
591 derived from CIRPAS Twin Otter and R/V Ronald H. Brown data and comparison with
592 observations, *Jour. Geophys. Res.: Atmos.*, 108(D23),
593 <https://doi.org/10.1029/2002JD003260>, 2003.
- 594 Curci, G., Hogrefe, C., Bianconi, R., Im, U., Balzarini, A., Baró, R., Brunner, D., Forkel, R.,
595 Giordano, L., Hirtl, M., Honzak, L., Jiménez-Guerrero, P., Knote, C., Langer, M., Makar,
596 P. A., Pirovano, G., Pérez, J. L., San José, R., Syrakov, D., Tuccella, P., Werhahn, J.,
597 Wolke, R., Žabkar, R., Zhang, J., and Galmarini, S.: Uncertainties of simulated aerosol
598 optical properties induced by assumptions on aerosol physical and chemical properties: An
599 AQMEII-2 perspective, *Atmos. Environ.*, 115, 541–552, 2015.
- 600 Ding, A.J., Huang, X., Nie, W., Sun, J.N., Kerminen, V.M., Petäjä, T., Su, H., Cheng, Y.F.,
601 Yang, X.Q., Wang, M.H. and Chi, X.G.: Enhanced haze pollution by black carbon in
602 megacities in China, *Geophys. Res. Lett.*, 43(6), pp.2873-2879,
603 <https://doi.org/10.1002/2016gl067745>, 2016.

604 Forkel, R., Balzarini, A., Baró, R., Bianconi, R., Curci, G., Jiménez-Guerrero, P., Hirtl, M.,
605 Honzak, L., Lorenz, C., Im, U., Pérez, J. L., Pirovano, G., José, R. S., Tuccella, P.,
606 Werhahn, J., and Zabkar, R.: Analysis of the WRF-Chem contributions to AQMEII phase2
607 with respect to aerosol radiative feedbacks on meteorology and pollutant distributions,
608 *Atmos. Environ.*, 115, 630–645, 2015. Gao, Y., Zhang, M., Liu, Z., Wang, L., Wang, P.,
609 Xia, X., Tao, M. and Zhu, L.: Modeling the feedback between aerosol and meteorological
610 variables in the atmospheric boundary layer during a severe fog–haze event over the North
611 China Plain, *Atmos. Chem. Phys.*, 15(8), pp.4279-4295, [https://doi.org/10.5194/acpd-15-](https://doi.org/10.5194/acpd-15-1093-2015)
612 1093-2015, 2015.

613 Gao, M., Carmichael, G.R., Wang, Y., Saide, P.E., Yu, M., Xin, J., Liu, Z. and Wang, Z.:
614 Modeling study of the 2010 regional haze event in the North China Plain, *Atmos. Chem.*
615 *Phys.*, 16(3), p.1673, <https://doi.org/10.5194/acpd-15-22781-2015>, 2016.

616 Gao, M., Carmichael, G.R., Wang, Y., Saide, P.E., Liu, Z., Xin, J., Shan, Y. and Wang, Z.:
617 Chemical and Meteorological Feedbacks in the Formation of Intense Haze Events, In *Air*
618 *Pollution in Eastern Asia: An Integrated Perspective* (pp. 437-452), Springer, Cham.,
619 https://doi.org/10.1007/978-3-319-59489-7_21, 2017.

620 Gao, M., Han, Z., Liu, Z., Li, M., Xin, J., Tao, Z., Li, J., Kang, J.E., Huang, K., Dong, X. and
621 Zhuang, B.: Air quality and climate change, Topic 3 of the Model Inter-Comparison Study
622 for Asia Phase III (MICS-Asia III)–Part 1: Overview and model evaluation. *Atmos. Chem.*
623 *Phys.*, 18(7), p.4859, <https://doi.org/10.5194/acp-18-4859-2018>, 2018a.

624 Gao, M., Ji, D., Liang, F. and Liu, Y.: Attribution of aerosol direct radiative forcing in China
625 and India to emitting sectors, *Atmos. Environ.*, 190, pp.35-42,
626 <https://doi.org/10.1016/j.atmosenv.2018.07.011>, 2018b.

627 Gao, M., Liu, Z., Zheng, B., Ji, D., Sherman, P., Song, S., Xin, J., Liu, C., Wang, Y., Zhang,
628 Q., Wang, Z., Carmichael, G., and McElroy, M.: China's Clean Air Action has suppressed
629 unfavorable influences of climate on wintertime PM_{2.5} concentrations in Beijing since
630 2002, *Atmos. Chem. Phys. Discuss.*, <https://doi.org/10.5194/acp-2019-325>, in review,
631 2019a.

632 Gao, M., Sherman, P., Song, S., Yu, Y., Wu, Z. and McElroy, M.B.: Seasonal prediction of
633 Indian wintertime aerosol pollution using the ocean memory effect, *Sci. Adv.*, 5(7),
634 p.eaav4157, <https://doi.org/10.1126/sciadv.aav4157>, 2019b.

635 Grell, G. A., Peckham, S. E., Schmitz, R., McKeen, S. A., Frost, G., Skamarock, W. C., and
636 Eder, B.: Fully coupled “online” chemistry within the WRF model, *Atmos. Environ.* 39,
637 6957–6975, 2005.

638 Han, Z.: Direct radiative effect of aerosols over East Asia with a regional coupled
639 climate/chemistry model, *Meteorologische Zeitschrift*, 19(3), pp.287-298,
640 <https://doi.org/10.1127/0941-2948/2010/0461>, 2010.

641 Han, Z., Li, J., Guo, W., Xiong, Z., and Zhang, W.: A study of dust radiative feedback on
642 dust cycle and meteorology over East Asia by a coupled regional climate-chemistry-
643 aerosol model, *Atmos. Environ.*, 68, 54–63,
644 <https://doi.org/10.1016/j.atmosenv.2012.11.032>, 2013.

645 Huang, J., Lin, B., Minnis, P., Wang, T., Wang, X., Hu, Y., Yi, Y. and Ayers, J.K.:
646 Satellite - based assessment of possible dust aerosols semi - direct effect on cloud water
647 path over East Asia, *Geophys. Res. Lett.*, 33(19), <https://doi.org/10.1029/2006GL026561>,

648 2006.

649

650 Huang, X., Ding, A., Liu, L., Liu, Q., Ding, K., Niu, X., Nie, W., Xu, Z., Chi, X., Wang, M.
651 and Sun, J.: Effects of aerosol-radiation interaction on precipitation during biomass-
652 burning season in East China, *Atmos. Chem. Phys.*, 16(15), [https://doi.org/10.5194/acp-](https://doi.org/10.5194/acp-2016-272)
653 2016-272, 2016.

654 Huang, X., Song, Y., Zhao, C., Cai, X., Zhang, H. and Zhu, T.: Direct radiative effect by
655 multicomponent aerosol over China, *Jour. Clim.*, 28(9), pp.3472-3495,
656 <https://doi.org/10.1175/JCLI-D-14-00365.1>, 2015.

657

658 Jacobson, M.Z., Kaufman, Y.J. and Rudich, Y.: Examining feedbacks of aerosols to urban
659 climate with a model that treats 3-D clouds with aerosol inclusions, *Jour. Geophys. Res.:*
660 *Atmos.*, 112(D24), <https://doi.org/10.1029/2007jd008922>, 2017.

661 Jia, R., Liu, Y., Hua, S., Zhu, Q. and Shao, T.: Estimation of the aerosol radiative effect over
662 the Tibetan Plateau based on the latest CALIPSO product, *Jour. Met. Res.*, 32(5), pp.707-
663 722, <https://doi.org/10.1007/s13351-018-8060-3>, 2018.

664 Li, M., Zhang, Q., Kurokawa, J.-I., Woo, J.-H., He, K., Lu, Z., Ohara, T., Song, Y., Streets, D.
665 G., Carmichael, G. R., Cheng, Y., Hong, C., Huo, H., Jiang, X., Kang, S., Liu, F., Su, H.,
666 and Zheng, B.: MIX: a mosaic Asian anthropogenic emission inventory under the
667 international collaboration framework of the MICS-Asia and HTAP, *Atmos. Chem. Phys.*,
668 17, 935–963, <https://doi.org/10.5194/acp-17-935-2017>, 2017.

669 Li, J., Han, Z., and Zhang, R.: Influence of aerosol hygroscopic growth parameterization on
670 aerosol optical depth and direct radiative forcing over East Asia, *Atmos. Res.*, 140-141,
671 14-27, <https://doi.org/10.1016/j.atmosres.2014.01.013>, 2014.

672 Li, Z., Lee, K.H., Wang, Y., Xin, J. and Hao, W.M.: First observation-based estimates of cloud-
673 free aerosol radiative forcing across China, *Jour. Geophys. Res.:* *Atmos.*, 115(D7),
674 <https://doi.org/10.1029/2009jd013306>, 2010.

675 Liu, Q., Jia, X., Quan, J., Li, J., Li, X., Wu, Y., Chen, D., Wang, Z. and Liu, Y.: New positive
676 feedback mechanism between boundary layer meteorology and secondary aerosol
677 formation during severe haze events, *Sci. rep.*, 8(1), p.6095,
678 <https://doi.org/10.1038/s41598-018-24366-3>, 2018.

679 Liu, Y., Huang, J., Shi, G., Takamura, T., Khatri, P., Bi, J., Shi, J., Wang, T., Wang, X. and
680 Zhang, B.: Aerosol optical properties and radiative effect determined from sky-radiometer
681 over Loess Plateau of Northwest China, *Atmos. Chem. Phys.*, 11(22), pp.11455-11463,
682 <https://doi.org/10.5194/acp-11-11455-2011>, 2011.

683 Liu, Y., Sato, Y., Jia, R., Xie, Y., Huang, J. and Nakajima, T.: Modeling study on the transport
684 of summer dust and anthropogenic aerosols over the Tibetan Plateau, *Atmos. Chem.*
685 *Phys.*, 15(21), pp.12581-12594, <https://doi.org/10.5194/acp-15-12581-2015>, 2015.

686

687 Lohmann, U. and Feichter, J.: Global indirect aerosol effects: a review, *Atmos. Chem.*
688 *Phys.*, 5(3), pp.715-737, <https://doi.org/10.5194/acp-5-715-2005>, 2005.

689 Peters-Lidard, C. D., Kemp, E. M., Matsui, T., Santanello Jr., J. A., Kumar, S. V., Jacob, J. P.,
690 Clune, T., Tao, W.-K., Chin, M., Hou, A., Case, J. L., Kim, D., Kim, K.-M., Lau, W., Liu,
691 Y., Shi, J., Starr, D., Tan, Q., Tao, Z., Zaitchik, B. F., Zavodsky, B., Zhang, S. Q., and

692 Zupanski, M.: Integrated modeling of aerosol, cloud, precipitation and land processes at
693 satellite-resolved scales, *Environ. Model. Softw.*, 67, 149–159,
694 <https://doi.org/10.1016/j.envsoft.2015.01.007>, 2015.

695 Qiu, Y., Liao, H., Zhang, R. and Hu, J.: Simulated impacts of direct radiative effects of
696 scattering and absorbing aerosols on surface layer aerosol concentrations in China during
697 a heavily polluted event in February 2014, *Jour. Geophys. Res.: Atmos.*, 122(11), pp.5955-
698 5975, <https://doi.org/10.1002/2016JD026309>, 2017.

699 Saide, P. E., Spak, S. N., Carmichael, G. R., Mena-Carrasco, M. A., Yang, Q., Howell, S.,
700 Leon, D. C., Snider, J. R., Bandy, A. R., Collett, J. L., Benedict, K. B., de Szoeke, S. P.,
701 Hawkins, L. N., Allen, G., Crawford, I., Crosier, J., and Springston, S. R.: Evaluating
702 WRF-Chem aerosol indirect effects in Southeast Pacific marine stratocumulus during
703 VOCALS-REx, *Atmos. Chem. Phys.*, 12, 3045-3064, <https://doi.org/10.5194/acp-12-3045-2012>, 2012.

705 Twomey, S.: Aerosols, clouds and radiation. *Atmospheric Environment. Part A. General*
706 *Topics*, 25(11), pp.2435-2442, [https://doi.org/10.1016/0960-1686\(91\)90159-5](https://doi.org/10.1016/0960-1686(91)90159-5), 1991.

707 Wang, H., Xue, M., Zhang, X.Y., Liu, H.L., Zhou, C.H., Tan, S.C., Che, H.Z., Chen, B. and
708 Li, T.: Mesoscale modeling study of the interactions between aerosols and PBL
709 meteorology during a haze episode in Jing–Jin–Ji (China) and its nearby surrounding
710 region–Part 1: Aerosol distributions and meteorological features, *Atmos. Chem.*
711 *Phys.*, 15(6), pp.3257-3275, <https://doi.org/10.5194/acp-15-3257-2015>, 2015.

712 Wang, J., Wang, S., Jiang, J., Ding, A., Zheng, M., Zhao, B., Wong, D.C., Zhou, W., Zheng,
713 G., Wang, L. and Pleim, J.E.: Impact of aerosol–meteorology interactions on fine particle
714 pollution during China’s severe haze episode in January 2013, *Env. Res. Let.*, 9(9),
715 p.094002, <https://doi.org/10.1088/1748-9326/9/9/094002>, 2014.

716 Wang, T., Li, S., Shen, Y., Deng, J., and Xie, M.: Investigations on direct and indirect effect
717 of nitrate on temperature and precipitation in China using a regional climate chemistry
718 modeling system, *J. Geophys. Res.*, 115, <https://doi.org/10.1029/2009JD013264>, 2010.

719 Wang, Z., Li, J., Wang, Z., Yang, W., Tang, X., Ge, B., Yan, P., Zhu, L., Chen, X., Chen, H.
720 and Wand, W.: Modeling study of regional severe hazes over mid-eastern China in January
721 2013 and its implications on pollution prevention and control, *Sci. China Earth*
722 *Sciences*, 57(1), pp.3-13, <https://doi.org/10.1007/s11430-013-4793-0>, 2014.

723 Wu, J., Bei, N., Hu, B., Liu, S., Zhou, M., Wang, Q., Li, X., Liu, L., Feng, T., Liu, Z., Wang,
724 Y., Cao, J., Tie, X., Wang, J., Molina, L. T., and Li, G.: Aerosol-radiation feedback
725 deteriorates the wintertime haze in North China Plain, *Atmos. Chem. Phys. Discuss.*,
726 <https://doi.org/10.5194/acp-2018-1288>, in review, <https://doi.org/10.5194/acp-19-8703-2019>, 2019.

728 Yang, Q., W. I. Gustafson Jr., Fast, J. D., Wang, H., Easter, R. C., Morrison, H., Lee, Y.-N.,
729 Chapman, E. G., Spak, S. N., and Mena-Carrasco, M. A.: Assessing regional scale
730 predictions of aerosols, marine stratocumulus, and their interactions during VOCALS-REx
731 using WRF-Chem, *Atmos. Chem. Phys.*, 11, 11951–11975, doi:10.5194/acp-11-11951-
732 2011, 2011.

733

734 Zhang, B., Wang, Y. and Hao, J.: Simulating aerosol–radiation–cloud feedbacks on
735 meteorology and air quality over eastern China under severe haze conditions in

736 winter, *Atmos. Chem. Phys.*, 15(5), pp.2387-2404, [https://doi.org/10.5194/acp-15-2387-](https://doi.org/10.5194/acp-15-2387-2015)
737 2015, 2015.

738 Zhang, X., Zhang, Q., Hong, C., Zheng, Y., Geng, G., Tong, D., Zhang, Y. and Zhang, X.:
739 Enhancement of PM_{2.5} Concentrations by Aerosol-Meteorology Interactions Over
740 China, *Jour. Geophys. Res.: Atmos.*, 123(2), pp.1179-1194,
741 <https://doi.org/10.1002/2017jd027524>, 2018.

742 Zhang, Y., Wen, X.Y. and Jang, C.J.: Simulating chemistry–aerosol–cloud–radiation–climate
743 feedbacks over the continental US using the online-coupled Weather Research Forecasting
744 Model with chemistry (WRF/Chem), *Atmos. Env.*, 44(29), pp.3568-3582,
745 <https://doi.org/10.1016/j.atmosenv.2010.05.056>, 2010.

746 Zhong, J., Zhang, X., Dong, Y., Wang, Y., Liu, C., Wang, J., Zhang, Y. and Che, H.: Feedback
747 effects of boundary-layer meteorological factors on cumulative explosive growth of PM
748 2.5 during winter heavy pollution episodes in Beijing from 2013 to 2016, *Atmos. Chem.*
749 *Phys.*, p.247, <https://doi.org/10.5194/acp-18-247-2018>, 2018.

750

751

752

753

754

755

756